

Modeling and Simulation of Aviation Engine Ignition Spark Frequency Disorder

Shi Xudong*, Li Hongguang, Wang Ruowen and Xu Meng

Aeronautical Automation College, Civil Aviation University of China, 2898 Jinbei Road, Dongli District, Tianjin, 300300, China

Abstract: Igniter is an important part of aircraft engine, which should be reliable to ensure safety. Spark frequency disorder is common fault to the aviation ignition device, and it is great hidden danger to the aircraft engine. To guarantee the safety and reliability of aviation igniter, the fault mechanism of the aviation ignition spark frequency disorder is researched in this paper. The factors which will result in spark frequency disorder are studied, and the mathematical model of the ignition circuit and circuit simulation are presented, which lays the foundation for the follow-up research on the design of aviation ignition and the fault diagnosis.

Keywords: Aviation ignition device, Failure mechanism, Mathematical model, Simulation, Spark frequency.

1. INTRODUCTION

Aviation ignition is one of the important parts of the aero-engine, which is the heart of the aircraft. And its function is to produce sparks to ignite gas mixture. Aviation igniter is mainly composed of three parts: the ignition exciter, ignition leads and ignition spark plugs. The major performance parameters of aviation ignition spark include spark frequency, spark energy and spark duration [1-3]. Spark frequency is a key factor affecting the safety of the igniter. For high energy ignition that long-playing with high frequency high voltage and large current can cause very big workload to igniter itself, which threatens the service life of the internal electronic components. So the aircraft maintenance manual have clear rules on all technical data of spark frequency, of which the working time of ignition switch is also limited, which also shows the importance of aviation ignition spark frequency in the field of civil aviation [4, 5].

According to the long-term maintenance experience of engineering maintenance personnel, it is found that the spark frequency disorders fault occurs in the ignition exciter, which mainly caused by three situations: 1) The high voltage rectifier device fails to work, in other words, rectifier diode suffers short or open; 2) The transformer winding suffers short circuit between the turns or the layers, resulting in the change of the transformer turns ratio; 3) Discharge tube breakdown voltage changes due to aging problem. Spark frequency disorders include three conditions: spark frequency decreases, misfiring (no spark) and spark frequency increases which rarely happens. In this paper, the

fault mechanism of the aviation ignition spark frequency disorder is researched. The Factors which will result in spark frequency disorder are studied, and the mathematical model of the ignition circuit and circuit simulation are presented, which lays the foundation for the follow-up research on the design of aviation ignition and the fault diagnosis [6].

2. WORKING PRINCIPLES OF THE IGNITER

Alternating-current high-energy ignition circuit structure of aero-engine is shown in Fig. (1), which is mainly composed of three parts: alternating-current voltage booster module, rectifier voltage-doubling energy storage module, discharge module [7, 8]. Power is supplied to the unit input connector from the 115-volt, 400-cycle source in the aircraft. Power is first led through a filter which blocks conducted noise voltage from feeding back into the airplane electrical system. In the secondary of the power transformer, an alternating voltage is generated and then to be rectified and multiplied to charge the storage capacitor. When this voltage reaches the predetermined level calibrated for the spark gap in the discharge tube *SG* (the control gap), the gap breaks down to make the spark plug discharge [9-11].

The detailed process is: During the first half-cycle this follows a circuit through the rectifier D_1 and the doubler capacitor C_1 in parallel with the series circuit of the storage capacitor C_2 and the doubler capacitor C_3 back to the power transformer, leaving the capacitor C_2 charged. During the second half-cycle when the polarity reverses, this circuit is blocked by rectifier. The flow of this puke is through ground to the rectifier D_1 , storage capacitor C_2 , doubler capacitor C_1 , and back to the power transformer, doubler capacitor C_3 in parallel with the series circuit of the storage capacitor C_2 and the doubler capacitor C_1 . No matter how the polarity of the induced voltage changes, the voltage of the storage capacitor C_2 remain the state of charging, with each pulse the storage

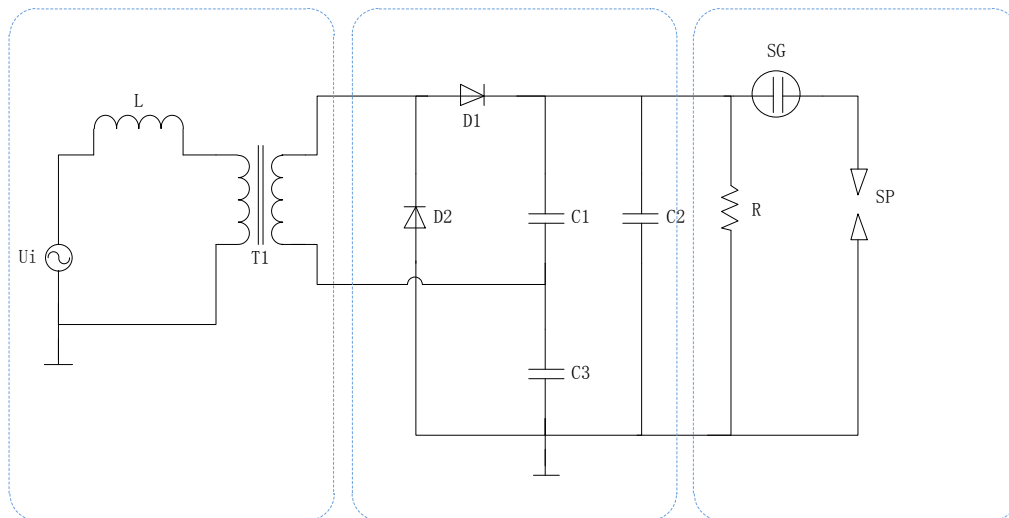


Fig. (1). Aviation ignition circuit.

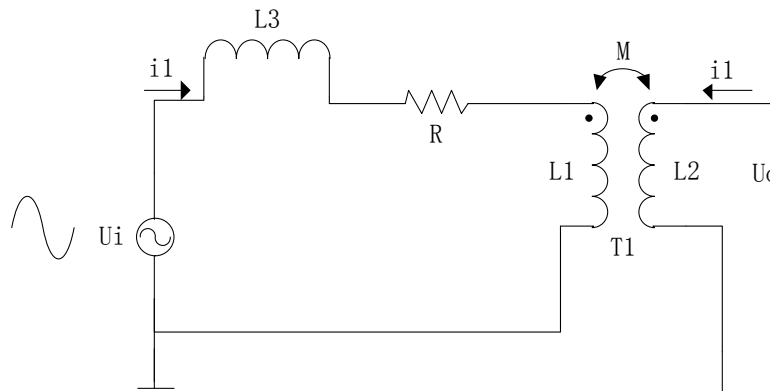


Fig. (2). Igniter AC booster circuit.

capacitor C_2 assumes a greater charge. After a certain times of cycles, the sum of the charge on the capacitor C_1 and C_3 approaches voltage approximately twice that generated in the power transformer. In this process, if the voltage on the C_2 rise to discharge tube SG threshold voltage (approximately 3000 volts), the discharge tube SG can be breakdown into the discharge process of spark plug with a strong spark discharge in the igniter, and the sparks ignite the gas mixture in the combustion chamber.

3. MATHEMATICAL MODELING OF THE AVIATION IGNITION CIRCUIT

3.1. The Calculation of AC Booster Module's Secondary Output Voltage

As shown in Fig. (1), the storage capacitor charging voltage is determined by the booster module. While as shown in Fig. (2), the booster module mainly includes the choke winding L_3 , winding equivalent resistance R and transformer T_1 (including primary winding inductance L_1 , secondary winding inductance L_2). In order to get the

mathematical relationship among the input voltage and the component parameters and the output voltage, and to find out the main components parameters affecting the output voltage, it is needed to build the corresponding mathematical model to the booster module, namely, to build explicit mathematical expression of output voltage with the input voltage and the parameters of the various components.

$$\begin{cases} \dot{U}_i^g = j\omega L_3 \dot{I}_1^g + R \dot{I}_1^g + j\omega L_1 \dot{I}_1^g + j\omega M \dot{I}_2^g \\ \dot{U}_o^g = j\omega L_2 \dot{I}_2^g + j\omega M \dot{I}_1^g \end{cases} \quad (1)$$

When there is no load in the secondary winding of the transformer, it matches this condition: $I_2 = 0$, $u_i = \sqrt{2}U_i \sin(\omega t + \varphi)$, and here U_i is the RMS (root-mean-square quantity) of the input voltage, $\omega = 2\pi f$. Assuming that $\varphi = 0$, put it into the equation (1), and the $u_o(t)$ can be obtained, as shown in equation (2).

$$u_o(t) = \sqrt{2} \frac{\omega M U_i}{\sqrt{R^2 + \omega^2(L_1 + L_3)^2}} \sin(\omega t + \theta), \quad (2)$$

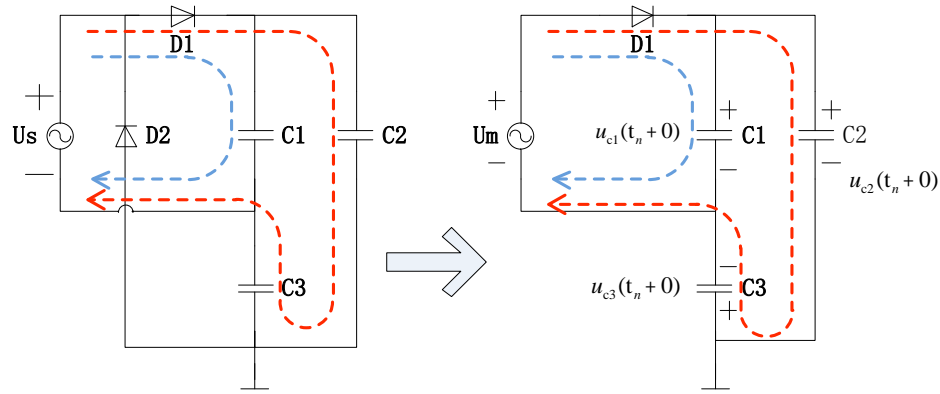


Fig. (3). Current direction of voltage rectifier circuit in positive half-cycle.

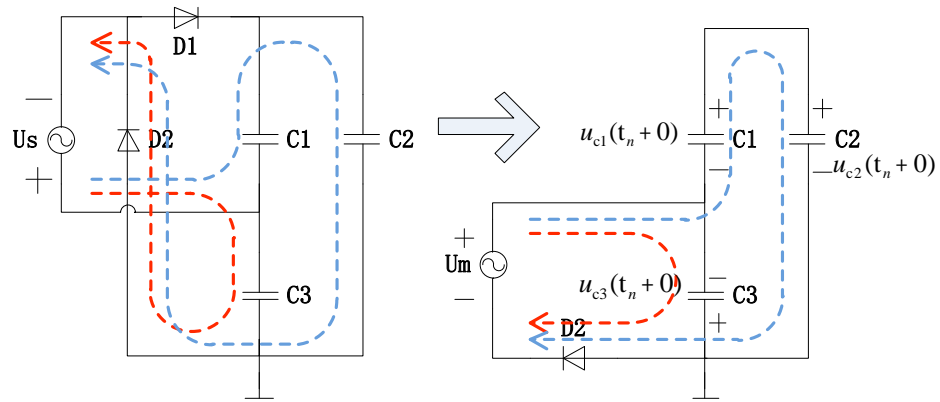


Fig. (4). Current direction of voltage rectifier circuit in negative half-cycle.

Where θ is the initial phase of the output voltage in transformer secondary winding. Assume that $U_m = \sqrt{2}\omega M U_i / \sqrt{R^2 + \omega^2(L_1 + L_3)^2}$, namely the peak output voltage of the secondary winding in transformer. Take η as transformer coupling coefficient, then $M = \eta\sqrt{L_1 L_2}$, and due to the equation $R \ll \omega(L_1 + L_3)$, $U_m \approx \eta\sqrt{2L_1 L_2} U_i / (L_1 + L_3)$. The parameters are: $f=400\text{Hz}$, $L_1=100\text{mH}$, $L_2=60\text{H}$, $U_i=115\text{V}$, $\eta=0.98$, $L_3=0.05\text{H}$.

3.2. Mathematical Modeling of Voltage Doubler and Energy Storage Circuit

In order to facilitate the analysis of the rectifier circuit, the diode of the rectifier is considered to be the ideal diode, namely, the forward conduction resistance is zero, the forward conduction voltage is zero, back resistance is infinite, and backward voltage is infinite. The sinusoidal voltage across the secondary winding of the transformer could be replaced with the square wave, which has the same cycle time and the same peak voltage as the sinusoidal

voltage of the secondary winding of the transformer. C_1, C_3 have the same capacitance (which can guarantee the function of voltage doubling), and each element voltage reference direction are shown in Fig. (3) and Fig. (4).

During $0: t_1$, the square wave is in the first half-cycle. As shown in Fig. (3), $U_s = U_m$, D_1 forward conducting, D_2 reverse cut-off, and assuming that there is no initial stored energy in the capacitor C_1, C_2, C_3 , $u_{c1}(0^-) = 0$. When $t = 0$, D_1 forward conducting, the voltage of the capacitor C_1 leap to the peak value of U_s , $u_{c1}(0^+) = U_m$. Given that C_2 is in series with C_3 , according to the law of capacitor in series, it is easy to get $u_{c2}(0^+), u_{c3}(0^+)$. During $t_1: t_2$, the square wave is in the second half-cycle when the polarity reverses, $U_s = -U_m$, D_1 reverse cut-off, D_2 forward conducting. When $t = t_1$, D_2 forward conducting, the voltage of the capacitor C_1, C_2, C_3 leap to new values, and the initial voltage of the capacitor C_1, C_2, C_3 respectively are: $u_{c1}(t_1 - 0) = u_{c1}(0^+)$, $u_{c2}(t_1 - 0) = u_{c2}(0^+)$, $u_{c3}(t_1 - 0) = u_{c3}(0^+)$.

Assuming that it is in the positive half cycle of the output voltage across the secondary winding of the transformer, according to the law of conservation of charge and the Kirchhoff's voltage law, equation (3) can be obtained.

$$\begin{cases} u_{c1}(0+) = U_m \\ u_{c1}(0-) = u_{c2}(0-) = u_{c3}(0-) = 0 \\ u_{c2}(0+) = C_3 / (C_2 + C_3) U_m \\ u_{c3}(0+) = C_2 / (C_2 + C_3) U_m \end{cases} \quad (3)$$

Afterward, during the odd numbered half-cycle, equation (4) can be obtained.

$$\begin{cases} u_{c1}(t_{2n} + 0) = U_m \\ u_{c2}(t_{2n} + 0) = \frac{1}{C_2} \int_{t_{2n}-0}^{t_{2n}+0} i_{c2}(t) dt + u_{c2}(t_{2n} - 0) \\ u_{c3}(t_{2n} + 0) = \frac{1}{C_3} \int_{t_{2n}-0}^{t_{2n}+0} i_{c2}(t) dt + u_{c3}(t_{2n} - 0) \\ u_{c2}(t_{2n} + 0) + u_{c3}(t_{2n} + 0) = U_m \end{cases} \quad (4)$$

During the even numbered half-cycle, equation (5) can be obtained.

$$\begin{cases} u_{c3}(t_{2n+1} + 0) = -U_m \\ -u_{c1}(t_{2n+1} + 0) + u_{c2}(t_{2n+1} + 0) = U_m \\ u_{c1}(t_{2n+1} + 0) = -\frac{1}{C_1} \int_{t_{2n+1}-0}^{t_{2n+1}+0} i_{c2}(t) dt + u_{c1}(t_{2n+1} - 0) \\ u_{c2}(t_{2n+1} + 0) = \frac{1}{C_2} \int_{t_{2n+1}-0}^{t_{2n+1}+0} i_{c2}(t) dt + u_{c2}(t_{2n+1} - 0) \end{cases} \quad (5)$$

After several cycles of the above circuit derivation, $u_{c2}(t_n+0)$ during each half-cycle can be obtained respectively ($n=0,1,2,3,\dots$). From the above analysis, the voltage of C_2 (voltage of energy-storage capacitor) can be obtained.

$$u_{c2}(t_n + 0) = 2\alpha \sum_{i=0}^n \beta^i U_m - \alpha \beta^n U_m \quad (6)$$

The parameters are: $C_1=C_3$, $\alpha=C_1/(C_1+C_2)=C_3/(C_2+C_3)$, $\beta=C_2/(C_1+C_2)=C_2/(C_2+C_3)$. And because $\alpha+\beta=1$, deform equation (6), and equation (7) can be obtained.

$$u_{c2}(t_n + 0) = 2U_m - (1 + \beta)\beta^n U_m \quad (7)$$

Furthermore, the expression of the voltage of C_2 at any time can be obtained.

$$u_{c2}(t) = 2U_m - (1 + \beta)\beta^{2\beta} U_m, \quad (8)$$

Where f is the frequency of the input voltage, and then the spark frequency can be obtained.

$$f_{sp} = 2f \frac{\lg \beta}{\lg \frac{2U_m - U_{br}}{(1 + \beta)U_m}} \quad (9)$$

Substituting the equation of U_m ($U_m \approx \eta \sqrt{2L_1 L_2} U_i / (L_1 + L_3)$) into equation (9).

$$f_{sp} = 2f \frac{\lg \beta}{\lg \frac{2\sqrt{2L_1 L_2} \eta U_i - (L_1 + L_3) U_{br}}{\sqrt{2L_1 L_2} (1 + \beta) U_i}} \quad (10)$$

The f_{sp} is the spark frequency needed in this paper, and U_{br} is the threshold of discharge tube SG, under the condition of $U_{br} < 2U_m$. Through the equation (10), it is found that the spark frequency f_{sp} shows a trend of increase with the increase of L_2 and β , and shows a trend of decrease with the increase of U_{br} . In this paper, the parameter are: $C_1=C_3=10nF$, $C_2=4\mu F$, $\beta=0.9975$.

4. SIMULATION OF SPARK FREQUENCY DISORDER

Aviation igniter constantly charge the energy storage capacitor in the process of rectification voltage doubling, this is a process of charge accumulation, which need some time to finish the whole work. But, as a matter of fact, the spark discharge stage is a strong spark discharge process, the accumulation of charge on the energy storage capacitor need instant release, which will produce high-energy sparks, and the discharge process is very short. The whole process for energy storage capacitor on the voltage transformation process is: after a slowly rising, the voltage of the storage capacitor reach to the max value (the threshold of the discharge tube), then breakdown, discharge tube voltage instantaneous reduced. So the discharge tube breakdown discharge action is a key link in the process of discharge frequency of aviation igniter, take the time slot from the moment of power on to the moment of discharge tube breakdown action as a discharge cycle. As for the situation of continuous discharge, take the time slot between twice breakdown actions of discharge tube as a discharge cycle. Thus the voltage change of the storage capacitor directly reflects the discharge cycle, from which spark frequency is known.

4.1. Fault Simulation of High Voltage Rectifier Device

Fault of rectifier device mostly happens to rectifier diode, and the typical faults are short circuit and open circuit.

Through the simulation results, as shown in Fig. (5), we can see that any high voltage rectifier diode happening open or short circuit fault will result in the energy storage capacitor failing to be normally charged to the threshold voltage of discharge tube, thus the discharge tube is unable to discharge, which means the spark frequency is 0 Hz. Failure of rectifier module will seriously affects the work of igniter, and if igniter cannot produces sparks, the aircraft engine cannot do ground ignition or re-ignition in the air.

4.2. Fault Simulation of Transformer Secondary Winding

In the process of aviation igniter maintenance, it is found that the circumstance that igniter transformer winding gets

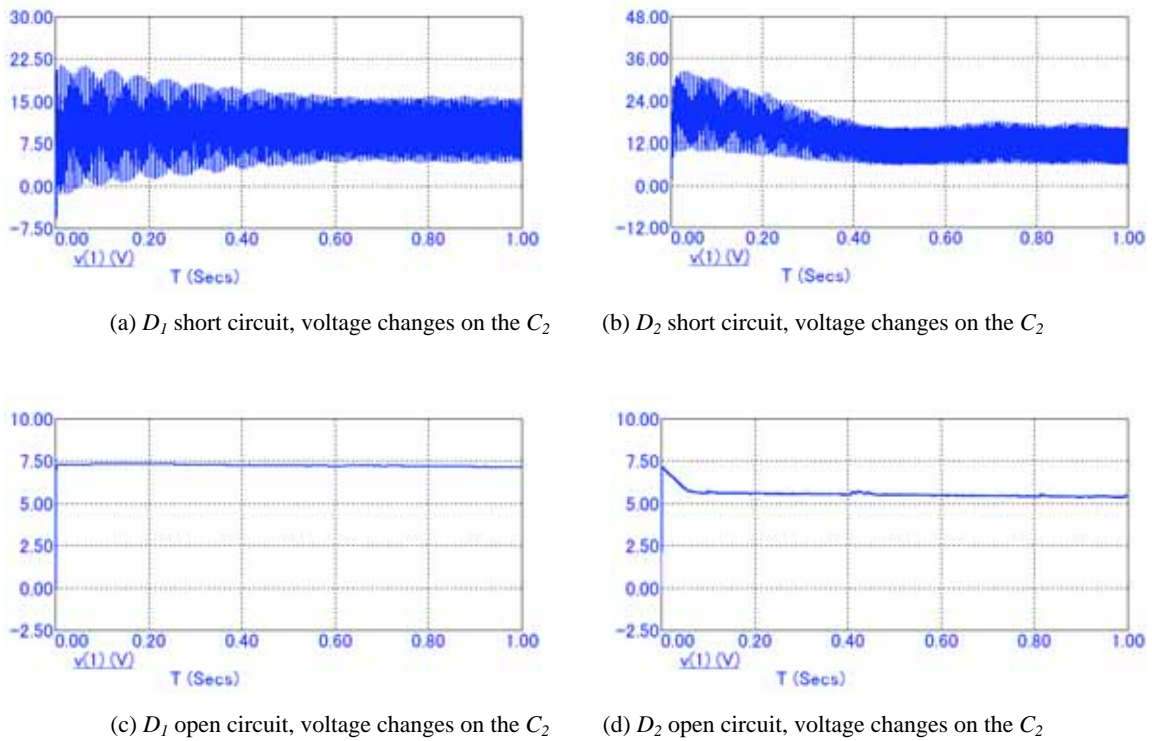


Fig. (5). High voltage rectifier diode failure lead to spark frequency disorders.

short circuit between the turns or layers mostly occurs on transformer secondary winding, which directly results in that the secondary winding inductance decreases, and what's more, the primary and secondary winding turns ratio decreases, leads to the decrease of U_m . The equation (9) shows that the decrease of U_m makes spark frequency f_{sp} decrease.

The Simulation results as shown in Fig. (6) shows that ignition transformer secondary windings appearing interturn or interlayer short circuit will significantly reduce the ignition spark frequency to the value below the normal one, or even cause the charging voltage being too low to make energy storage capacitor be charged to the threshold voltage of discharge tube, lead to be unable to discharge. Because in the practical application of air igniter it does not appears for primary winding of the primary transformer to failure, here the primary winding fault type is not considered. If secondary winding circuit goes open, it will also lead to the ignition's failure, which means the spark frequency is 0 Hz.

4.3. Fault Simulation of Breakdown Voltage Increase Due to Discharge Tube Ageing

Due to frequent high voltage breakdown discharge, discharge characteristic of discharge tube may have changes. The common changes include: breakdown voltage increases, breakdown voltage decreases, and even the discharge tube is completely damaged and fail to discharge. As one of the common faults, breakdown voltage rise is focused on here [12].

In the simulation results, as shown in Fig. (7), when the threshold voltage of discharge tube increases as a result of aging, spark frequency obviously decreases, even when the energy storage capacitor are full charged, discharge tube still fails to be breakdown to ignite, which seriously affects the normal work of the aircraft igniter.

CONCLUSION

In this paper, the mathematical model on the rectifying energy-storing circuit of the AC type aviation ignition is built, and the mathematical expression of the spark frequency with each components parameters of the ignition circuit is deduced, and then based on the mathematical model, the circuit simulation of the way how the changing parameters of the ignition circuit infect the spark frequency is implemented. It is concluded that: 1) Open or short in any of the high voltage rectifier diode will cause the rectifying failures, which can't charge the energy storage capacitor; 2) Short circuit between the turns or the layers in the transformer secondary winding, leads to the change of the transformer turns ratio and the reduction of charging voltage, which results in the extension of the energy storage capacitor charging time and even is unable to charge to the threshold voltage of the discharge tube, which ultimately reduces the spark frequency or even produces no ignition sparks; 3) The discharge tube aging causes the threshold voltage changed in the process of using aviation igniter, which makes the energy storage capacitor discharge earlier or later, and then leading to spark frequency disorder.

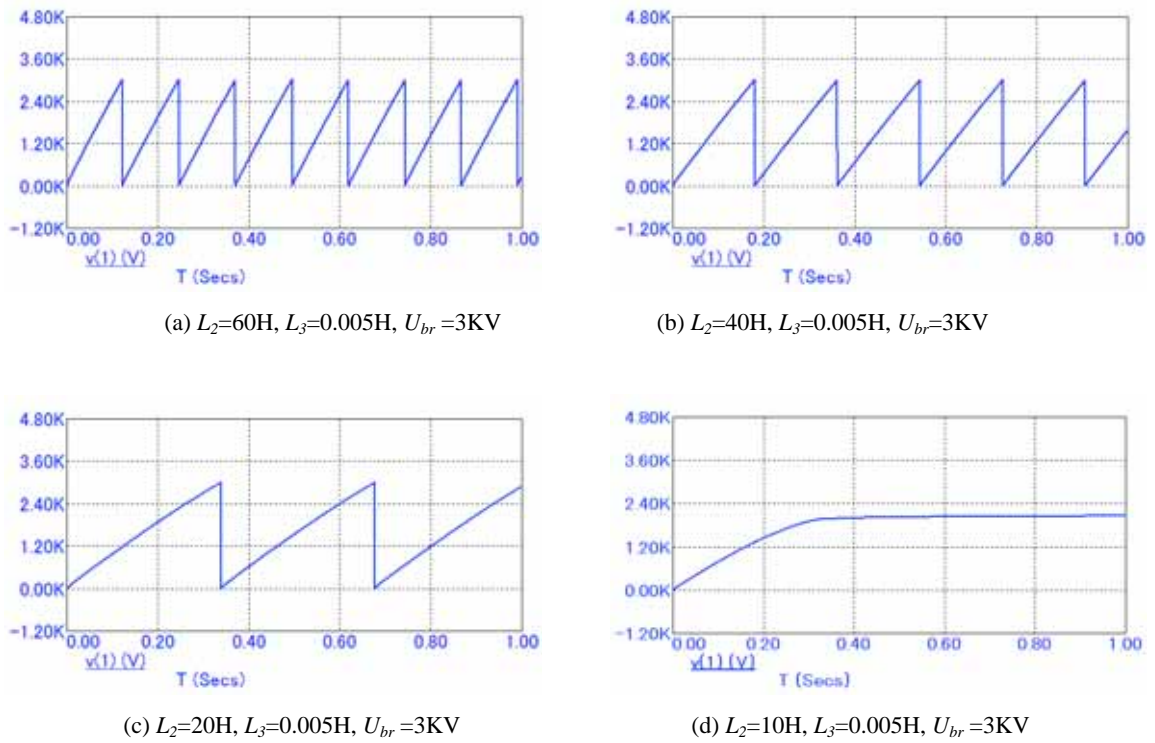


Fig. (6). Failure of transformer secondary winding leading spark frequency disorders.

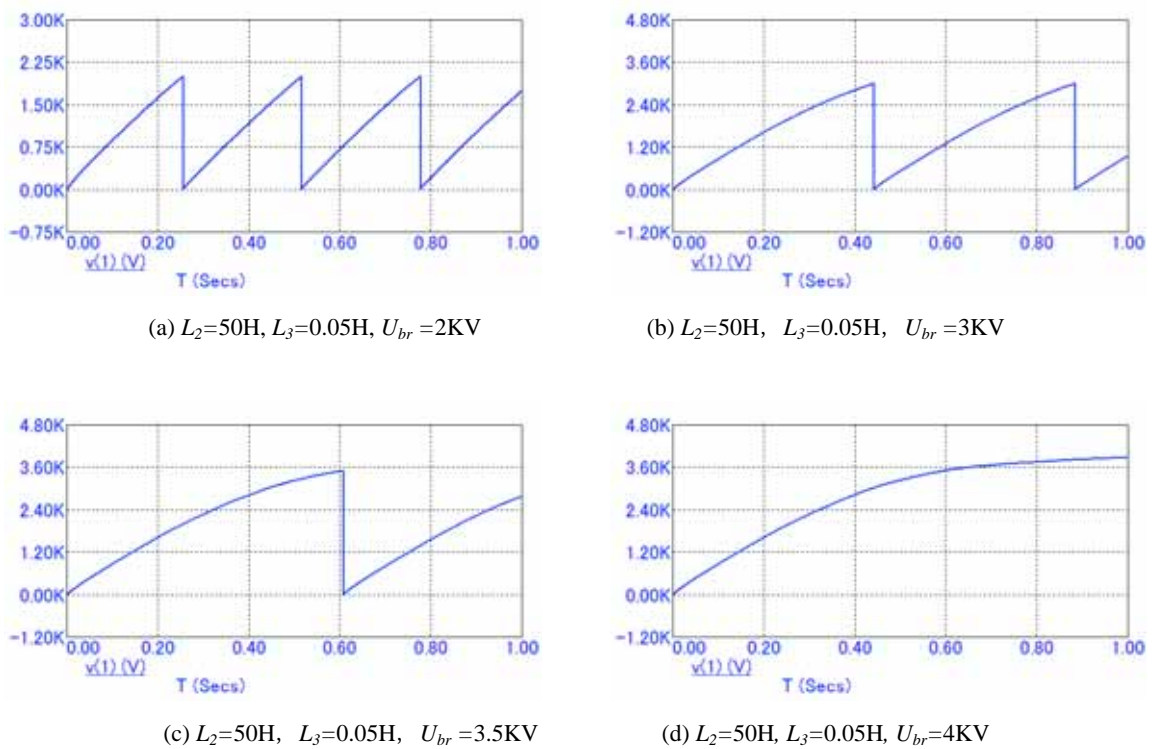


Fig. (7). Discharge tube failure resulting in spark frequency disorders.

CONFLICT OF INTEREST

The authors confirm that this article content has no conflict of interest.

ACKNOWLEDGEMENTS

This work is supported by National Natural Science Foundation of China (Grant No. #U1233201); Important &

Specific Projects of Civil aviation science and technology project, Fundamental Research Project of the Central Universities (Grant No. #ZXH2012B002 & No. #3122013-P005).

REFERENCES

- [1] K. Song, Z. Y. Gao, and J. B. Liao, "Modeling and simulation of switching power supply of aviation ignition device," *Journal of System Simulation*, vol. 18, no. 057, pp. 4991-4997, 2008.
- [2] J. Zhao, and T. Zhang, "Study on spark frequency stability of aeroengine transistor ignition system," *Modern Electronics Technique*, vol. 11, no. 037, pp. 116-118, 2013.
- [3] X. Shi, G. Ren, J. Li, and S. Zhang, "Fault diagnosis method research of aircraft ignition system based on waveform image matching," *Procedia Engineering*, vol. 15, pp. 2527-2532, 2011.
- [4] S. Chen, J. Rong, G. Bi, X. Li, and R. Cao, "Spectrum comparative study of commutation failure and short-circuit fault in UHVDC transmission system," *TELKOMNIKA (Telecommunication Computing Electronics and Control)*, vol. 12, no. 4, pp. 753-762, 2014.
- [5] A. Triwiyatno, "Engine torque control of spark ignition engine using fuzzy gain scheduling," *TELKOMNIKA (Telecommunication Computing Electronics and Control)*, vol. 10, no. 1, pp. 83-90, 2012.
- [6] L. Tian, X. Li, C. Liu, X. Shi, and L. Wang, "Design of fault diagnosis system for aircraft engine ignition component," *Journal of Civil Aviation University of China*, vol. 31, no. 4, pp. 6-9, 2013.
- [7] J. R. Berliner, J. C. Driscoll, S. J. Kempinski, and T. S. Wilmot, "Turbine Engine Ignition Exciter Circuit Including Low Voltage Lockout Control," U.S. Patent No. 5,852,381 (Patent) 1998.
- [8] D. P. Mahajan, R. Narayanswamy, and S. K. Saxena, "Novel exciter circuit for ignition of gas turbine engines in aerospace applications," In: *IEEE International Conference on Industrial Technology*, pp. 613-617, 2013.
- [9] Y. Jang, and M. M. Jovanovic, "Interleaved boost converter with intrinsic voltage-doubler characteristic for universal-line PFC front end", *IEEE Transactions on Power Electronics*, vol. 22, no. 4, pp. 1394-1401, 2007.
- [10] W. Wen, W. Wang, and D. Zhang, "Design and realization of multiple-voltage rectifier used in image intensifier," *Computer Simulation*, vol. 7, no. 086, pp. 343-346, 2009.
- [11] W. J. Lee, C. E. Kim, G. W. Moon, and S. K. Han, "A new phase-shifted full-bridge converter with voltage-doubler-type rectifier for high-efficiency PDP sustaining power module", *IEEE Transactions on Industrial Electronics*, vol. 55, no. 6, pp. 2450-2458, 2008.
- [12] F. Tian, D. Long, Q. Pan, and Y. Huang, "Study of high energy ignition gas discharge tubes of electrical properties," *Vacuum Electronics*, vol. 6, no. 015, pp. 53-55, 2010.

Received: October 16, 2014

Revised: December 23, 2014

Accepted: December 31, 2014

© Xudong *et al.*; Licensee Bentham Open.

This is an open access article licensed under the terms of the Creative Commons Attribution Non-Commercial License (<http://creativecommons.org/licenses/by-nc/3.0/>) which permits unrestricted, non-commercial use, distribution and reproduction in any medium, provided the work is properly cited.